

A Simple Picosecond Pulse Generator Based on a Pair of Step Recovery Diodes

Lianfeng Zou, Shulabh Gupta, Christophe Caloz

Abstract—A picosecond pulse generator based on a pair of step recovery diodes (SRD), leveraging the transient response of the SRD PN junction and controlling the pulse width by a resistor, is proposed. We first explain the operation principle of the device, decomposing the pulse generation into different phases, and then demonstrate an experimental prototype with two different resistance, and hence pulse width, values.

Keywords—UWB pulse generator, real-time analog signal processing (R-ASP), step recovery diode (SRD)

I. INTRODUCTION

The emerging Real-time Analog Signal Processing (R-ASP) technology [1], using dispersion-engineered structures (analog signal processors) providing specified group delays versus frequency responses for processing high-frequency and wide-bandwidth signals in real time, may lead to novel low-cost and low-complexity radio systems [2] for future millimeter wave and terahertz wireless communications.

Analog signal processors usually deal with ultra-short pulses with very rich spectral contents. Such pulses may be generated by different techniques [3]. Among them, the step recovery diode (SRD) approach [4]–[6] features simple circuit design, while providing picosecond pulse generation capability. Conventional SRD-based pulse generators usually employ an SRD to generate a pulse with picosecond rising edge, which destructively interferes with its opposite-polarity delayed replica produced by a short-circuited stub, which results in a short pulse whose width is equal to the round trip time along the stub. However, the stub configuration suffers from spurious reflections in both forward and backward directions, whose suppression requires pulse shaping networks [6], and requires complicated tuning schemes [7].

In this paper, we propose a stub-less pulse generator based on a pair of SRDs, which is immune of spurious reflections and which provides flexible control of the pulse width via a simple resistance.

II. PRINCIPLE

The transient behaviour of a PN junction in response to a step voltage from the forward to the reverse bias regimes is shown in Fig. 1. Initially, the PN junction is forward biased with current i_F . When the voltage v_i reverses polarity, the junction is not switched off immediately, but rather takes time τ_1 (storage phase), with current $i_{R,transient}$, to neutralize the charges stored in the depletion region and progressively raise the junction barrier [8]. Note that during the whole

storage phase, the junction maintains low resistance, and almost constant junction voltage, i.e. $v_j \approx V_T$. Near the end of the storage phase, the raising junction barrier increases the resistance, finally switching off the junction for a decay time τ_2 (decay phase), which is extremely short (in picosecond range) for an SRD [8]. Assuming constant i_F and constant $i_{R,transient}$, the storage phase time is given by [8]

$$\tau_1 = \tau_L \ln \left(1 + \frac{i_F}{i_{R,tran}} \right), \quad (1)$$

where τ_L is the minority carrier lifetime. We shall next present our pulse generator based on this SRD transient physics.

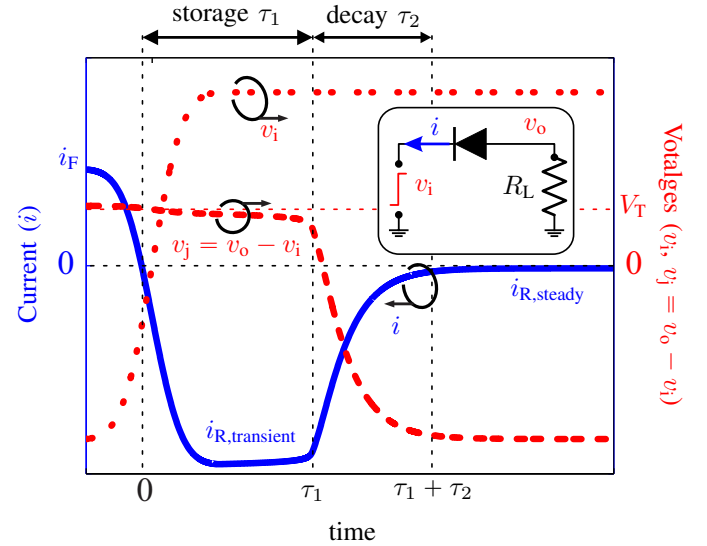


Fig. 1: PN junction transient current i (solid blue) and junction voltage v_j (dash red) in response to a step voltage v_i (dot red) from the forward to the reverse bias regimes.

Figure 2 shows the schematic of the proposed SRD-pair pulse generator. The generator is triggered by the rising edge of the input voltage through PIN diode D1, that is always ON for blocking possible negative input voltages. Its core is the parallel connection of SRDs D2 and D3, biased at their cathode by DC $V_s < 0$ through R_1 current limiter, with R_2 controlling the pulse width, as will be shown later. Finally, Schottky diode D4, operates as a pulse formation switch. The resistor $R_0 = 50 \Omega$ ensures input matching during the pulse production. Assuming square-wave (0-2.5 V) excitation v_1 , the operation may be decomposed into 5 phases, shown in Fig. 3.

- Phase 1 ($t < t_1$): D2 and D3 are forward biased, and

L. Zou (lianfeng.zou@polymtl.ca) and C. Caloz are with Polytechnique Montréal, Montréal, Québec, Canada.

S. Gupta is with Carleton University, Ottawa, Ontario, Canada.

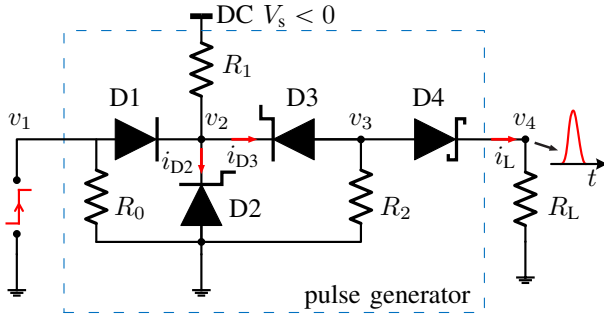


Fig. 2: Proposed SRD-pair pulse generator.

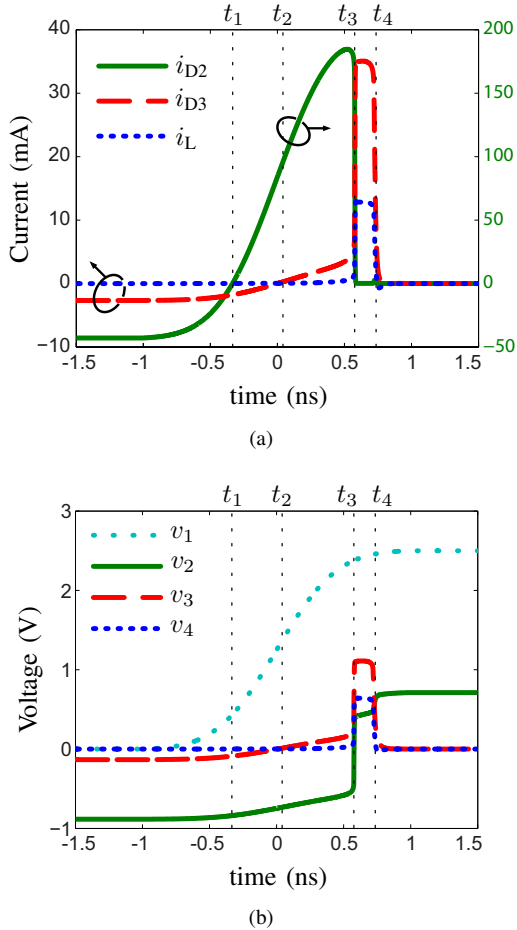


Fig. 3: Circuit simulated (a) currents (polarities referred to current directions indicated in Fig. 2) and (b) voltages, with $V_s = -3.5$ V, $R_1 = 25$ Ω , $R_2 = 50$ Ω , and Spice models for the diodes in Table. I.

D4 is off. The excitation v_1 is close to 0 V, so the D2 and D3 forward currents are such that $i_{F,D2} \gg i_{F,D3}$ due to the existence of R_2 in the D3 loop. The junction voltages $v_{j,D2} = -v_2$ and $v_{j,D3} = v_3 - v_2$, where $v_3 < 0$ due to the current flowing in

TABLE I: Diodes used in the generator with reference to Fig. 2.

Notation	Model
D1	Avago Tech. HMPS-2822
D2	Aeroflex MMDB30-0805
D3	Aeroflex MMDB30-0805
D4	Skyworks SMS7630-061-0201

R_2 from the ground to node 3, so that D4 is off and $v_4 = 0$.

- Phase 2 ($t_1 < t < t_2$): D2 is in storage regime, D3 is still forward biased, and D4 is still off. The excitation v_1 starts rising, driving D2 ($i_{R,D2} > 0$) into storage regime before D3 due to the smaller resistance in the D2 current loop than that in the D3 one and hence faster current changing rate ($\partial i_{D2}/\partial t > \partial i_{D3}/\partial t$) in response to the rising edge of v_1 . According to Fig. 1, $v_{j,D2} = -v_2$ varies only slightly in storage regime, and $v_3 < 0$ because D3 is still forward biased, and hence keeping D4 off.

- Phase 3 ($t_2 < t < t_3$): D2 and D3 are both in storage regime, D4 is still off. The voltage v_1 eventually also drives D3 into storage regime ($i_{R,D3} > 0$). Since $i_{F,D2}/i_{R,D2} \ll i_{F,D3}/i_{R,D3}$, we have $\tau_{1,D2} < \tau_{1,D3}$ according to (1), and therefore D2 will switch off before D3. In the meanwhile, v_3 follows v_2 , with insufficient variation to switch D4 on.

- Phase 4 ($t_3 < t < t_4$): D2 is off, D3 is still in storage regime, D4 is on. The SRD D2 abruptly switches off at t_3 , while D3 remains in storage regime. Consequently, v_2 , and following v_3 , abruptly increase, which switches D4 on, and therefore generates at the output the rising edge of v_4 . Moreover, the off-switching of D2, and the on-switching of D4, which makes R_L parallel to R_2 , together boost $i_{R,D3}$, starting to shorten the D3 storage time, which would otherwise be longer as expected in Phase 3.

- Phase 5 ($t > t_4$): D2, D3, D4 are all off. The D3 storage phase suddenly ends at t_4 , nullifying $i_{R,D3}$ and v_3 , and hence switching D4 off, which results in the falling edge of v_4 .

When the input level goes back to zero, the generator returns to the regime of Phase 1, waiting for the next voltage step to resume the aforementioned pulse formation cycle.

Let us now examine the factors determining the pulse width. Equation (1) assumes constant $i_{R,transient}$ over the entire storage phase τ_1 . As explained above, the storage phase for D3 is from t_2 to t_4 . However, since $i_{R,D3}(t_2 < t < t_3) \ll i_{R,D3}(t_3 < t < t_4)$, and $i_{R,transient}$ in (1) should be replaced by $i_{R,D3}(t_3 < t < t_4)$ for the effective storage time of D3. Since this interval ($[t_3, t_4]$) corresponds to the pulse duration, this duration can be approximated as

$$T \approx \tau_L \ln \left[1 + \frac{i_{F,D3}}{i_{R,D3}(t_3 < t < t_4)} \right]. \quad (2)$$

with an accuracy that is proportional to $i_{R,D3}(t_2 < t < t_3)$ and hence inversely proportional to R_2 , i.e. the closer $i_{R,D3}$ to zero in the interval $[t_2, t_3]$ (associated with larger R_2), the better the accuracy, as will be shown later in Fig. 4(a). Using Ohm

law, one may further write (2) in the form

$$T \approx \tau_L \ln \left(1 + r \frac{R_2 || R_L}{R_2} \right) = \tau_L \ln \left(1 + r \frac{R_L}{R_2 + R_L} \right), \quad (3)$$

where r is the ratio of v_3 in the forward bias regime to v_3 in the $[t_3, t_4]$ interval. Equation (3) reveals that, for given R_L , one may adjust R_2 to control the pulse width. This is confirmed by the simulation result in Fig. 4(a), which also show the result for the approximation in (2). Finally, Fig. 4(b) plots the pulse magnitude, which is seen to be essentially flat versus R_2 .

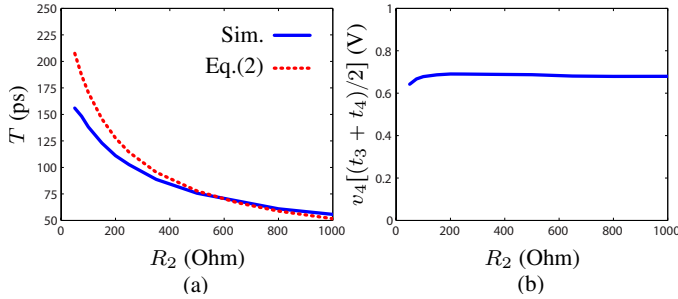


Fig. 4: (a) Circuit simulated half-magnitude pulse width (solid blue) and calculated pulse width (dash red) by (2) (with simulated currents and $\tau_L = 3$ ns [9]) versus R_2 . (b) Circuit simulated pulse magnitude.

III. EXPERIMENTAL DEMONSTRATION

Figure 5 shows the fabricated prototype, whose diode models are listed in Table. I, and where R_1 consists in two 0805 150 Ω resistors in parallel, R_0 is a 0603 50 Ω resistor, and R_2 is a 0603 50 or 560 Ω resistor. The experimental results are shown in Fig. 6 (solid red). The half-magnitude pulse widths are 94 and 62 ps for $R_2 = 50 \Omega$ and 560 Ω , respectively, which are different from the corresponding simulation pulse widths in Fig. 4(a). Ringing tails are also observed. To understand the cause of the pulse width discrepancy between simulation and experiment and the experimental ringing tails, one should note that the transmission line lengths are assumed to be zero in Fig. 2 and in the corresponding simulation results in Fig. 3 and Fig. 4. However, in the fabricated prototype, nonzero-length transmission lines delay the multiple internal reflections between diodes, which are not perfectly matched, hence generating successive replicas of the intended output pulse corresponding to the ringing tail. Moreover, the spurious pulses may constructively or destructively interfere with the main one, resulting in wider or shorter pulse width compared to the simulated on in Fig. 4(a). One may confirm this explanation by including finite-length transmission lines in the simulation circuit, as shown by the dash-blue curves in Fig. 6. In practice, one may naturally improve the output pulse shape by enhancing the matching of the diodes and using the shortest possible interconnecting lines.

IV. CONCLUSION

A simple pulse generator based on a pair of SRDs with pulse width adjustable by a single resistor is presented, analyzed and

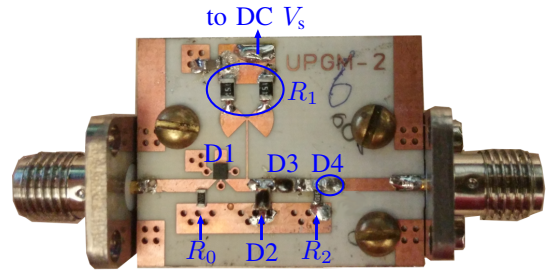


Fig. 5: Experimental prototype.

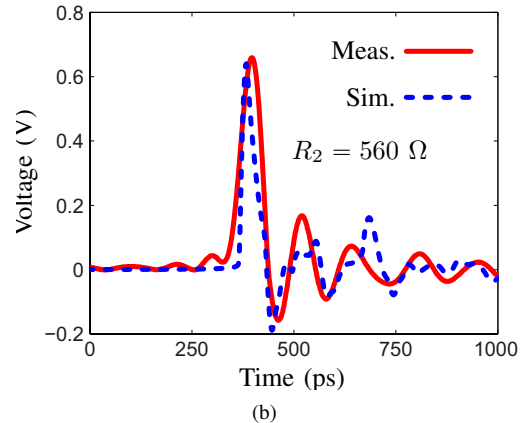
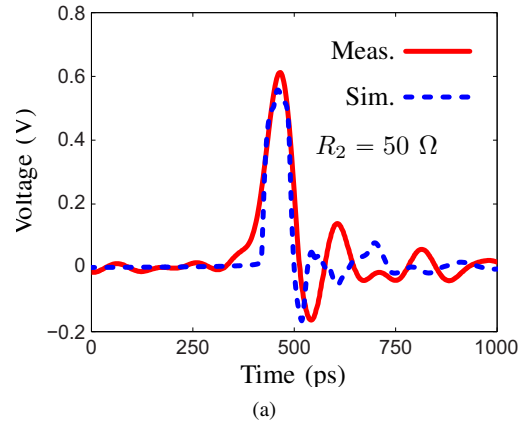


Fig. 6: Experimental (solid red) and circuit simulation (with finite-length transmission lines) (dash blue) results corresponding to (a) $R_2 = 50 \Omega$ and (b) $R_2 = 560 \Omega$, ($V_s = -3.5$ V and $v_i = 0/2.5$ V).

experimentally demonstrated. Such a pulse generator may find wide applications in R-ASP and other UWB radio systems with low cost and low complexity.

REFERENCES

- [1] C. Caloz, S. Gupta, Q. Zhang, and B. Nikfal, "Analog signal processing: A possible alternative or complement to dominantly digital radio schemes," *IEEE Microw. Mag.*, vol. 14, no. 6, pp. 87 – 103, Sep. 2013.

- [2] L. Zou, S. Gupta, and C. Caloz, "Dispersion code modulation for enhanced spectral efficiency in wireless communications,," in *IEEE AP-S Int. Antennas Propag. (APS)*, Fajaro, Puerto Rico, Jun. 2016, pp. 1851 – 1852.
- [3] J. R. Andrews, "Picosecond pulse generation techniques and pulser capabilities," Picosecond pulse labs, Tech. Rep., 2008.
- [4] A. Kamal, A. Bhattacharya, M. Tamrakar, and C. Roy, "Low-ring and reduced-cost step recovery diode based uwb pulse generators for gpr applications," *Microw. Opt. Technology Lett.*, vol. 56, no. 10, pp. 2289 – 2294, Oct. 2014.
- [5] J. S. Lee, C. Nguyen, and T. Scullion, "New uniplanar subnanosecond monocycle pulse generator and transformer for time-domain microwave applications," *IEEE Trans. Microw. Theory Techn.*, vol. 49, no. 6, pp. 1126 – 1129, Jun. 2001.
- [6] T. Xia, A. S. Venkatachalam, and D. Huston, "A high-performance low-ringing ultrawideband monocycle pulse generator," *IEEE Trans. Instrum. Meas.*, vol. 61, no. 1, pp. 261 – 266, Jan. 2012.
- [7] C. Zhang and A. E. Fathy, "Reconfigurable pico-pulse generator for uwb applications," in *IEEE MTT-S Int. Microw. Symp. (IMS)*, San Francisco, CA, Jun. 2006, pp. 407 – 410.
- [8] D. Tse and P. Viswanath, *Fundamentals of Wireless Communication*. New York, NY, USA: Cambridge University Press, 2005.
- [9] *Silicon Step Recovery Diodes*, Aeroflex Inc., 2005.